eISSN 2005-5447
International Journal of Stem Cells Vol. 13, No. 1, 2020 https://doi.org/10.15283/ijsc19088

ORIGINAL ARTICLE

miR-450a-5p Eliminates MGO-Induced Insulin Resistance via Targeting CREB

Cuifeng Wei*, Li Meng*, Yuting Zhang

Department of Endocrinology, Jingmen No. 1 People's Hospital, Jingmen, China

Background and Objectives: miR-450a-5p was involved in fat formation, however, its role in insulin resistance remains unclear. This study investigated the effects of miR-450a-5p on endothelial cells, with the aim of finding a potential target for diabetes mellitus.

Methods and Results: Human umbilical vein endothelial cells (HUVECs) were treated with low-glucose, high-glucose, methylglyoxal (MGO), and insulin alone or in combination with MGO. The expression of miR-450a-5p in treated cells was measured by quantitative real-time polymerase chain reaction (qRT-PCR) assays. The cell activity, migration and fat formation were determined by MTT experiments, Transwell assay and oil red O staining. The expressions of eNOS/AKT pathway-related proteins in cells were assessed by Western blot (WB) analysis. Furthermore, the target gene of miR-450a-5p was analyzed by double-luciferase reporter analysis, and its effects on eNOS/AKT pathway were estimated. We found that the expression of miR-450a-5p was decreased obviously in endothelial cells treated with high-glucose and MGO. *In vitro* cell experiments showed that MGO could not only promote the activity of endothelial cells, but also accelerate cell migration and fat accumulation, which, however, could be reversed by up-regulation of miR-450a-5p. Moreover, MGO inhibited eNOS/AKT pathway activation and NO release mediated by insulin, and such effects were reversed by up-regulation of miR-450a-5p. Furthermore, CREB was the target gene for miR-450a-5p, had an activation effect on the eNOS/AKT pathway.

Conclusions: Up-regulated miR-450a-5p eliminates MGO-induced insulin resistance via targeting CREB, and therefore could be used as a potential target to improve insulin resistance and treat patients with diabetes-related diseases.

Keywords: miR-450a-5p, Methylglyoxal, Insulin resistance, High-glucose, eNOS/AKT pathway

Introduction

As a common metabolic disorder, diabetes mellitus (DM) is characterized by chronically raised blood glucose caused by insulin dysfunction (1). Methylglyoxal (MGO) plays a pivotal role in the occurrence and development of DM, which is a highly active dicarbonyl compound and a ubiquitous product of cell metabolism (2). Concretely, MGO is an inherent by-product of glycolysis with cell permeability, the aggregation of MGO is harmful, as it is the most active compound to induce glycosylation products in cells (3), and this will induce insulin resistance to further aggravate pathoglycemia and dyslipidemia, thus promoting the progress of the disease (4). In addition, MGO can easily react with proteins, fats and nucleic acids to form

Received: July 15, 2019, Revised: November 21, 2019,
Accepted: December 30, 2019, Published online: February 29, 2020
Correspondence to **Yuting Zhang**
Department of Endocrinology, Jingmen No. 1 People's Hospital, No. 168, Xiangshan Avenue, Jingmen 448000, China
Tel: +86-0724-2305120, Fax: +86-0724-2305984
E-mail: yutingzh_zhang@163.com
*These authors contributed equally to this work.

advanced glycation end products, leading to the occurrence of cataract, retinopathy, kidney disease, vascular disease and other diabetic complications (5-8). In recent years, although several MGO scavengers have been discovered, effective clinical strategy for treating insulin resistance induced by MGO is still not available (9). Therefore, finding new targets to reduce MGO-induced insulin resistance may have a positive significance in improving the vascular function of DM.

MicroRNAs (miRNAs) are a class of single-stranded non-coding RNAs with length of approximately 18～23 nucleotides, and exert post-transcriptional modification through binding to the 3'untranslated region of target gene to affect the stability and translation of mRNA. It has shown that miRNAs account for about 1% of the genome of nuclear organisms, and their target genes regulate 30% of all genes (10). A recent study has found that miRNAs play an important role in the pathogenesis of DM by regulating the synthesis, secretion and signal transduction of insulin (11). Li (12) indicated that miR-375 regulates the expressions of insulin secretion-related genes to control the progression of DM. In addition, some scholars have found that miRNAs, such as miR-143, miR-145 and miR-29, also exert a vital function in insulin signaling pathway and insulin resistance. In related fields, miR-450a-5p can secrete various factors to regulate fat formation through paracrine signals (13). Correlatively, previous animal studies have shown that the formation of fat may be associated with the onset of DM (14). Nevertheless, the role and mechanism of miR-450a-5p in insulin resistance of endothelial cells remains unclear.

The relationship between miR-450a-5p and MGO was studied, and we further analyzed the effects and mechanisms of miR-450a-5p on MGO-induced human umbilical vein endothelial cells (HUVECs), including cell activity, migration, fat formation and insulin resistance. The aim of this study was to further analyze the action mechanism of miR-450a-5p in the insulin resistance induced by MGO in order to provide a potential target for related therapies, thus delaying the progression of DM and improving the prognosis of patients.

Materials and Methods

Cell culture and treatment

HUVECs were purchased by the American Type Culture Collection (ATCC, Rockville, MD, USA) and cultivated in EGM-2 Bullet Kit from Lonza (Walkersville, MD, USA). The cells were starved in medium containing with 0.25% albumin bovine serum (BSA) for 16 h and then respectively treated by low-glucose (5 mmol/L; Sigma, St Louis, USA), high-glucose (25 mmol/L; Sigma, St Louis, USA), and low-glucose combined with xylose (4.5 mmol/L; Sigma, St Louis, USA) for 24, 48, 72 h. In addition, different concentrations of MGO (0, 250, 500, 1000 μmol/L; Sigma, St Louis, USA) were added into HUVECs for 16 h, respectively. For comparison, cells were also pre-disposed with aminoguanidine bicarbonate salt (AG; 4 mmol/L; Sigma, St Louis, USA), and then treated by 500 μmol/L MGO for 16 h. Furthermore, insulin (100 nmol/L; Eli Lilly Florence, Italy) alone or in combined with MGO (500 μmol/L) were added into HUVECs for 10 min. For comparison, untreated cells (0 μmol/L) served as controls. Quantitative real-time polymerase chain reaction (qRT-PCR) assay was performed in treated HUVECs to determine the expression level of miR-450a-5p.

Cell transfection

Cell transfection was conducted in HUVECs in order to determine the effects of miR-450a-5p in HUVECs. Mimic control, miR-450a-5p mimic (#miR10001545-1-5, RiboBio, Guangzhou, China), inhibitor control, miR-450a-5p inhibitor (#miR20001545-1-5, RiboBio, Guangzhou, China), mimic plus negative control, and mimic combined with CREB (NM_009952.2, Han Bio, Shanghai, China) were separately transfected into MGO-treated cells. Moreover, miR-450a-5p mimic was also transfected into HUVECs after co-treatment with MGO and insulin. Lipofectamine^{TM} 2000 transfection reagent (Invitrogen, Carlsbad, California, USA) was used for cell transfection according to manufacturer's instructions.

qRT-PCR assay

The expression levels of relevant mRNAs in HUVECs were measured by qRT-PCR assays. Concretely, total RNA was separated from HUVECs using TRIzol reagent (Invitrogen, Carlsbad, California, USA). NanoDrop-2000c spectrophotometer (Thermo Fisher Scientific, Massachusetts, USA) was used to determine the amount of RNA, and the integrity was determined by 1% agarose modified gel electrophoresis. Then, 1 μg of separated RNA was reverse transcribed into cDNA with the PrimeScript RT Master Mix Perfect Real Time (TaKaRa, Shiga, Japan) according to the manufacturer's instructions. qRT-PCR assay was conducted using SYBR green qPCR assay (BioRad, USA) on the ABI Prism 7500 Fast Real-time PCR System (Applied Biosystems, Foster City, CA) following the reaction conditions: 30 cycles of hot start at 94℃ for 1 min, denaturation at 94℃ for 1 min, annealing at 50℃ for 45 s, and elongation at 72℃ for 2 min, then final elongation at 7

2℃ for 8 min. The sequences of primers were showed in Table 1 and synthesized by Gene Pharma (Shanghai, China). GAPDH or U6 served as internal reference, and the data were processed by the comparative $2^{-\Delta\Delta Ct}$ method (15).

Cell viability

MTT assay was carried out to measure the viability of transfected HUVECs. Briefly, HUVECs were seeded in 96-well plates (1×10^4 cells/well). After co-treated with MGO and transfection, 20 μL MTT reagent (Sigma, USA) was added at 24, 48, and 72 h to determine the viability of cells, and the optical densities (OD) value was read at 570 nm using the ELX-800 Biotek plate reader (Winooski, USA).

Transwell assay

A 24-well Transwell chamber (Corning, MA, USA) was performed to detect the migration ability of HUVECs after the MGO treatment and transfection. In brief, the lower chamber was supplemented with media containing 10% fetal bovine serum (FBS; Gibco, USA). Resuspended HUVECs (5×10^4 cells) were moved into the upper chambers and cultured for 24 h. Then, migrated cells were fixed by methanol and stained with the 0.1% crystal violet solution for 15 min. Nikon Eclipse TS-100 inverted microscope (Tokyo, Japan) was used for observation.

Oil red O staining

Fat accumulation in HUVECs was detected by oil red O staining. Cells were washed by phosphate buffer saline (PBS) and fixed by 10% formaldehyde at room temperature for 10 min. After the MGO treatment and transfection, HUVECs were incubated with 0.5% Oil red O solution (Gibco, USA) for 15 min, and then washed by water for 5 min. Stained HUVECs were photographed and viewed under DP73 Olympus microscope (Tokyo, Japan).

Griess reaction

NO in HUVECs culture medium was measured by Griess reaction. After the treatment and transfection, cell culture medium was collected, and the supernatant fraction after centrifugation (1000 g, 15 min) was taken as a sample solution for the measurement of NO using Nitrate/nitric Assay Kit Colorimetric (Sigma, USA). The assay used contained a chromophoric azo-derivative that allows NO to be detected at 540～570 nm by the microplate reader (Spectra MAX190; MD, USA).

Double-luciferase reporter analysis

Targetscan 7.2 (http://http://www.targetscan.org/.) predicted that CREB was the potential target for miR-450a-5p. For determination, double-luciferase report system detection kit (Promega, Madison, Wisconsin, USA) was used for double-luciferase reporter analysis. Briefly, HUVECs were seeded in 24-well plates (1×10^5 cell/well) for 24 h. Then, miR-450a-5p mimic or blank control was transfected into HUVECs combined with wild type CREB (CREB-WT) or its mutant type (CREB-MUT) using Lipofectamine™ 2000. After 48 h, the cells were lysed and the luciferase activity was evaluated with the GloMax® Discover Multimode Microplate Reader (GM3000, Promega, USA).

Western blot (WB) analysis

The expressions of related proteins in HUVECs were measures by WB assays. Total proteins of cells were separated by the RIPA buffer (Solarbio, Beijing, China), and Bicinchoninic Protein Assay kit (BCA, Pierce, Rockford, IL, USA) was used for quantitation. 30 μg of total protein was isolated using the sodium dodecyl sulfate polyacrylamide gel electrophoresis (SDS-PAGE, Beyotime, Shanghai, China), and moved onto the polyvinylidene fluoride (PVDF) membranes. Then, 5% non-fat dried milk was used to seal the membranes for 2 h. Primary antibodies including p-eNOS (1 : 2000, ab184154, Abcam, USA), p-eNOS (1 : 1000, ab138430, Abcam, USA), eNOS (1 : 1000, ab76198, Abcam, USA), p-Akt (1 : 1000, #9271, Cell Signalling Technology, USA) and Akt (1 : 1000, #9272, Cell Signalling Technology, USA) were subsequently used to incubated the membranes overnight at 4℃. GAPDH (1 : 1000, ab8245, Abcam, USA) served as the internal control. Subsequently, the homologous secondary antibodies goat anti-rabbit IgG H&L (HRP; 1 : 7000, ab97051, Abcam, USA) and goat anti-mouse IgG H&L (HRP; 1 : 1000,

Table 1. Primer base sequence

Gene	Forward (5′-3′)	Reverse (5′-3′)
miR-450a-5p	CGATCGGTTTTGCGATGTGTTCC	ATCCAGTGCAGGGTCCGAGG
CREB	TGCCACATTAGCCCAGGTA	GCTGTATTGCTCCTCCCT
GAPDH	AGAAGGCTGG GGCTCATTTG	AGGGGCCATC CACAGTCT TC
U6	CTCGCTTCGGCAGCACA	AACGCTTCACGAATTTGCGT

ab150113, Abcam, USA) were added for another 1 h at room temperature. The bands were developed by an enhanced chemiluminescence-detecting kit (Thermo Fisher, MA, USA).

Statistical analysis

Statistical Package of the Social Sciences 20.0 software (SPSS, Inc., Chicago, USA) was used for data analysis. The data were shown as mean±standard deviation (SD).

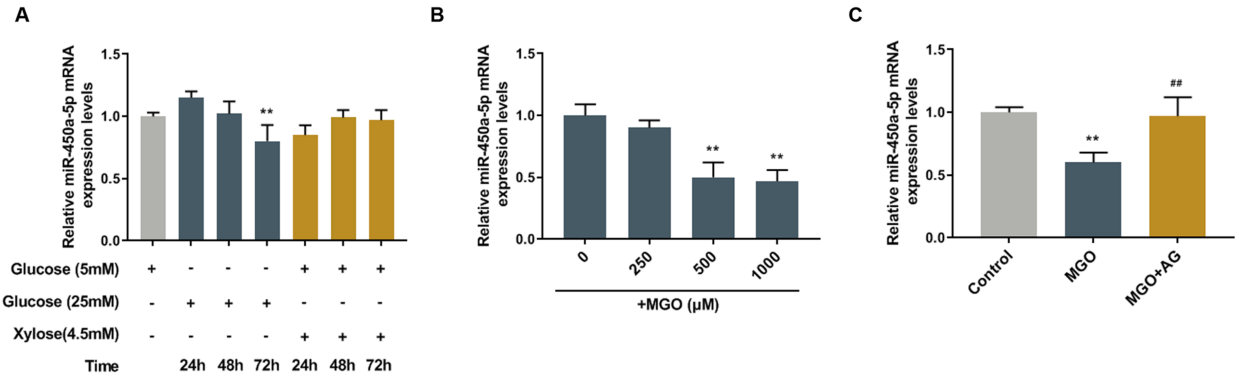

Fig. 1. Methylglyoxal (MGO) down-regulated the expression of miR-450a-5p in human umbilical vein endothelial cells (HUVECs). (A) Quantitative real-time polymerase chain reaction (qRT-PCR) assay measured the expression of miR-450a-5p in HUVECs after treatment with low-glucose (5 mM), high-glucose (25 mM), or low-glucose combined with xylose (4.5 mM) for 24, 48, 72 h. (B) qRT-PCR assay determined the expression of miR-450a-5p in HUVECs treated by different concentrations of MGO (0, 250, 500, 1000 μM). (C) qRT-PCR assay determined the expression of miR-450a-5p in HUVECs treated by control, MGO only or combined with aminoguanidine bicarbonate salt (AG). **p<0.001, vs. low-glucose, 0 μm, or Control; ##p<0.001, vs. MGO. n=3.

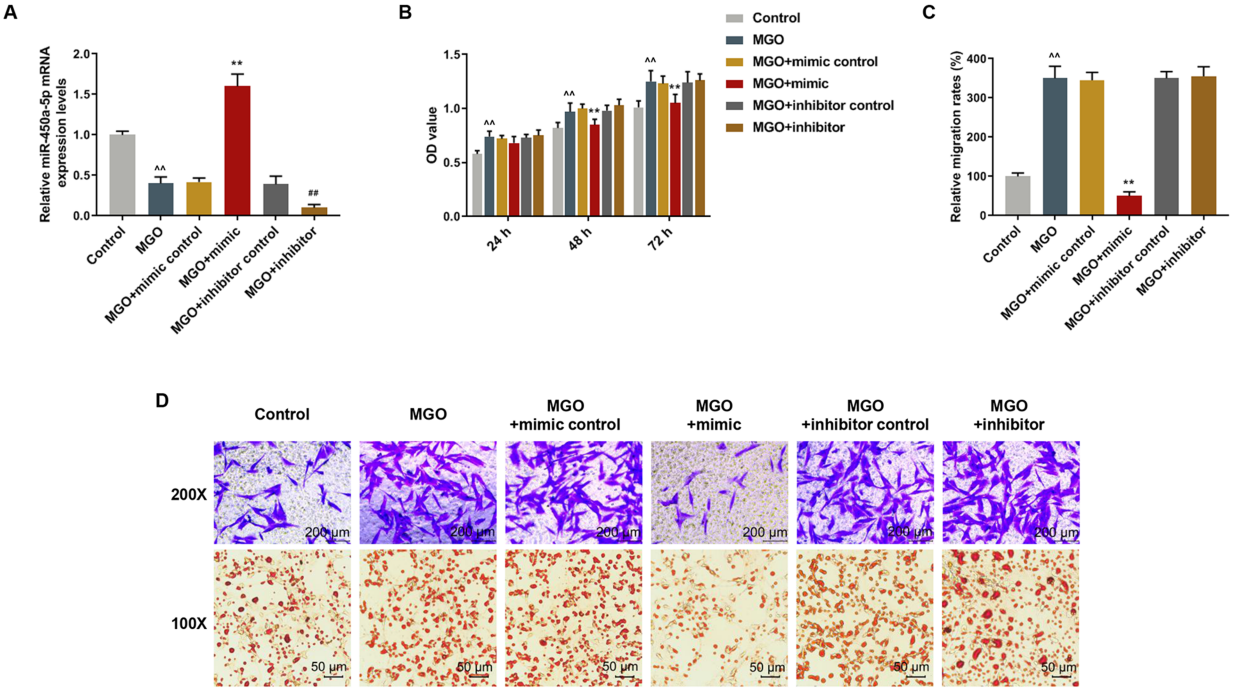

Fig. 2. Over-expressed miR-450a-5p inhibited viability, migration, and lipid formation of methylglyoxal (MGO)-induced human umbilical vein endothelial cells (HUVECs). Mimic control, miR-450a-5p mimic, inhibitor control, and miR-450a-5p inhibitor were respectively transfected into MGO-treated HUVECs. (A) Quantitative real-time polymerase chain reaction (qRT-PCR) assay measured the expression of miR-450a-5p in MGO-treated HUVECs after the transfection. (B) MTT assay detected the optical densities (OD) values of MGO-induced HUVECs after the transfection for 24, 48 and 72 h. (C) Quantitative analysis of Transwell assay in MGO-treated HUVECs after the transfection. (D) Microscopic images of Transwell and Oil red O staining experiments in MGO-induced HUVECs after transfection. ^^p<0.001, vs. Control; **p<0.001, vs. MGO+mimic control; ##p<0.001, vs. MGO+inhibitor control. n=3.

The comparison between groups was performed by Student's *t*-test or one-way analysis of variance (ANOVA) followed by Turkey's post-hoc test. All experiments were repeated in triplicate. $p<0.05$ was considered as statistically significant.

Results

Over-expressed miR-450a-5p inhibited viability, migration, and lipid formation of MGO-induced HUVECs

Based on qRT-PCR analysis, the expression level of miR-450a-5p in HUVECs was observably down-regulated after 72 h of high-glucose treatment ($p<0.001$), while low-glucose had no obvious effect on miR-450a-5p expression (Fig. 1A). Moreover, the expression of miR-450a-5p was obviously inhibited by adding MGO in HUVECs but reversed by AG ($p<0.001$; Fig. 1B and 1C). In order to further investigate the effects of miR-450a-5p and MGO on the cells, transfection was performed in the MGO-induced cells. The results revealed that miR-450a-5p was obviously up-regulated by mimic but was down-regulated by inhibitor ($p<0.001$; Fig. 2A), showing that the transfection was successful. Interestingly, MTT results showed that over-expressed miR-450a-5p prominently suppressed cell viability of MGO-induced HUVECs after transfection for 48 and 72 h ($p<0.001$; Fig. 2B), while down-regulated miR-450a-5p had no significant effect on cell viability. In transwell assay, microscopic and quantitative analyses showed that over-expressed miR-450a-5p observably suppressed the migration of MGO-induced HUVECs ($p<0.001$; Fig. 2C and 2D), whereas down-regulated miR-450a-5p had no significant effect on the migration. In the oil red O staining, lipid formation showed an orange color. From experimental images, we observed that over-expressed miR-450a-5p significantly reduced the lipid accumulation of MGO-induced HUVECs (Fig. 2D), while the lipid accumulation of cells was still high after down-regulating miR-450a-5p.

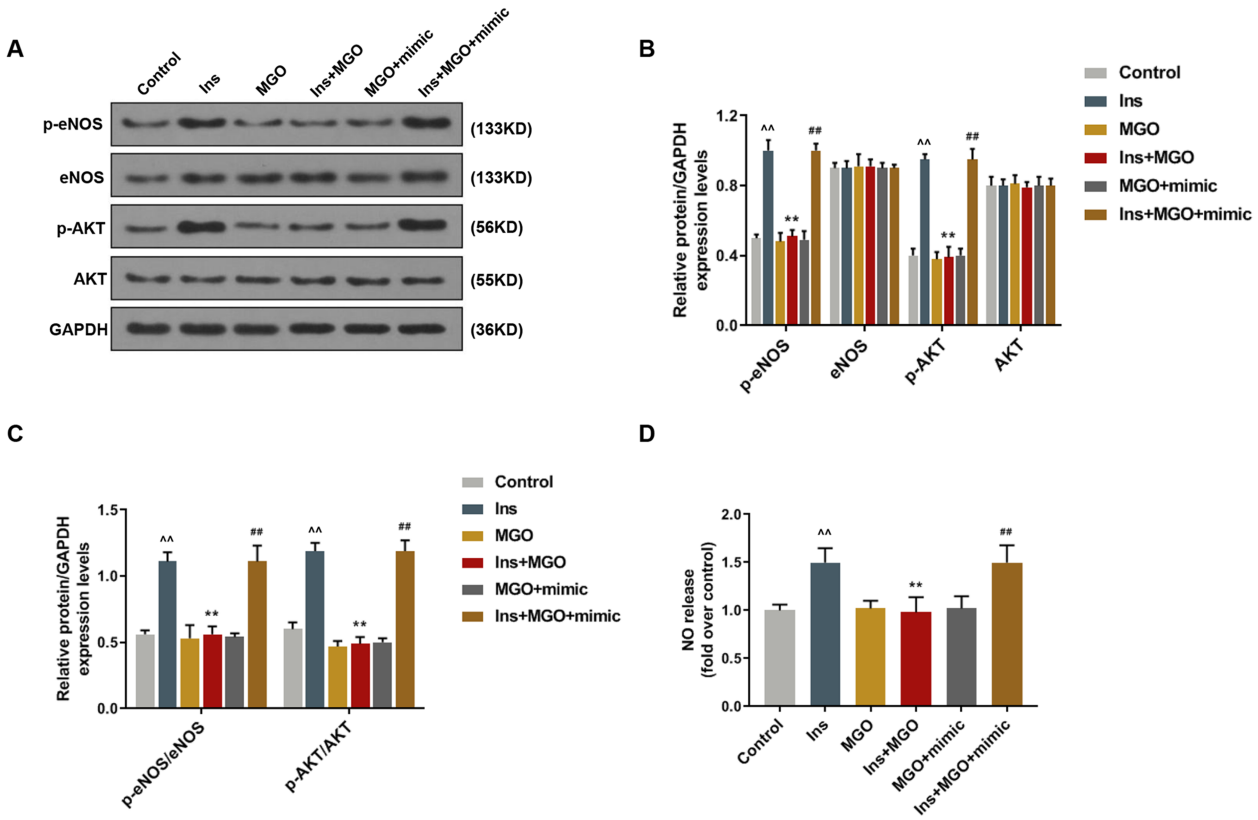

Fig. 3. Over-expressed miR-450a-5p inhibited the insulin resistance of methylglyoxal (MGO)-induced human umbilical vein endothelial cells (HUVECs). In this figure, HUVECs were respectively treated by control, insulin (Ins), MGO, insulin combined with MGO, miR-450a-5p mimic plus MGO, or mimic plus MGO and insulin. (A~C) Western blot (WB) bands and quantitative analysis determined the expressions of eNOS/AKT pathway-related proteins in HUVECs. (D) Griess reaction assessed the release of NO in HUVECs. ^^$p<0.001$, vs. Control; **$p<0.001$, vs. Ins; $^{\#\#}p<0.001$, vs. Ins+MGO. $n=3$.

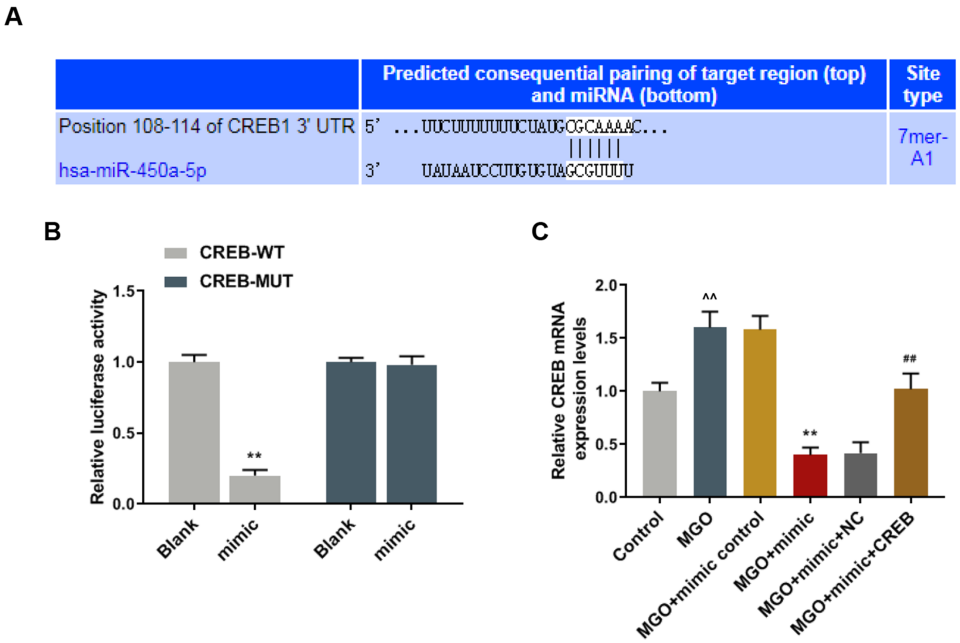

Fig. 4. CREB was the target gene for miR-450a-5p. (A) Targetscan7.2 predicted that the position 108-114 of CREB1 3'UTR was the binding site of miR-450a-5p. (B) Double-luciferase reporter analysis measured the luciferase activity of human umbilical vein endothelial cells (HUVECs) after transfection with miR-450a-5p mimic plus wild type CREB (CREB-WT) or its mutant type (CREB-MUT). (C) Quantitative real-time polymerase chain reaction (qRT-PCR) assay measured the expression of CREB in methylglyoxal (MGO)-induced HUVECs after transfection with mimic control, miR-450a-5p mimic, mimic plus negative control (NC) or CREB. ^^$p<0.001$, vs. Blank, or Control; **$p<0.001$, vs. MGO+mimic control; $^{\#\#}p<0.001$, vs. MGO+mimic+NC. n=3.

Over-expressed miR-450a-5p reduced the insulin resistance of MGO-induced HUVECs by targeting CREB

WB analysis suggested that the phosphorylation of eNOS and AKT was promoted by insulin but was reversed by MGO, and adding miR-450a-5p decreased the effects of MGO on eNOS/AKT pathway ($p<0.001$; Fig. 3A~C). Analogously, Griess reaction displayed that MGO inhibited the insulin-induced NO release but the effect as such could be relieved by up-regulated miR-450a-5p ($p<0.001$; Fig. 3D).

Targetscan7.2 predicted that the position 108-114 of CREB1 3'UTR was the binding site of miR-450a-5p (Fig. 4A). Double-luciferase reporter analysis indicated that the luciferase activity of HUVECs was decreased observably after the co-transfection with miR-450a-5p and CREB-WT, suggesting that CREB was the target gene for miR-450a-5p ($p<0.001$; Fig. 4B). Moreover, MGO promoted the mRNA expression of CREB in HUVECs, whereas miR-450a-5p had the completely opposite effect ($p<0.001$; Fig. 4C). As for the effects of CREB on eNOS/AKT pathway, WB experiment revealed that the up-regulation of CREB reduced the phosphorylation of eNOS/AKT pathway in HUVECs induced by insulin ($p<0.001$; Fig. 5).

Discussion

MGO can be obtained from food or produced in the body. *In vivo*, the main pathway of MGO production is glycolysis, and its content is abnormally increased by DM or hyperglycemia (16). MGO can be self-cleared by the body under normal physiological conditions, as MGO is characterized by hyper-responsiveness and short half-life, and the human body contains a variety of enzymes degrading MGO (17). In abnormal conditions, the dysfunction of MGO clearing pathway will lead to the gradual accumulation of MGO content, which can not only directly cause damage to cells, but also induce the massive generation of advanced glycation end products in the body (3). In previous studies, miRNAs such as miR-30b (18), miR-214 (19), miR-9a-3p (20) have been proved to be closely related to the content of MGO. In this study, the expression of miR-450a-5p, which showed a down-regulated trendency in HUVECs in high-glucose status, was also decreased with the increase of MGO concentration. Therefore, it can be speculated that miR-450a-5p might participate in the glycolysis process and play a role in the pathogenesis of DM.

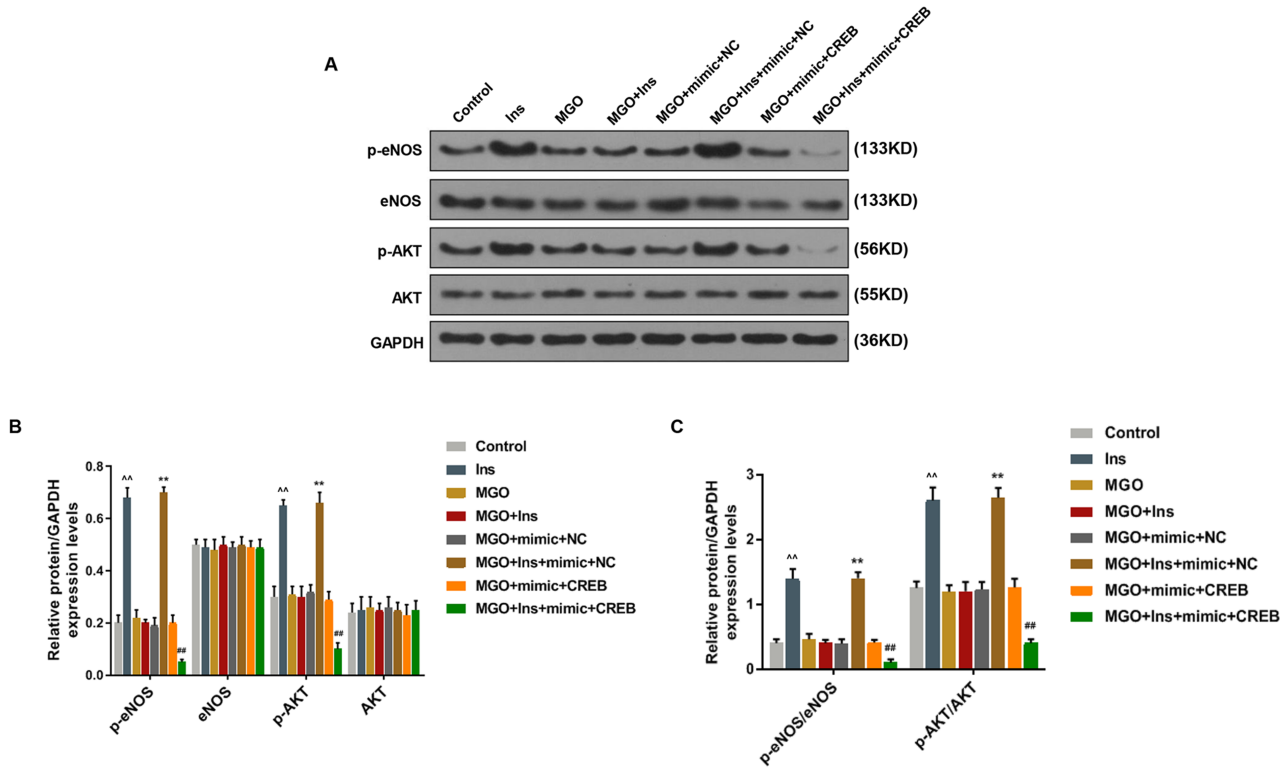

Fig. 5. Over-expressed miR-450a-5p reduced the insulin resistance of methylglyoxal (MGO)-induced human umbilical vein endothelial cells (HUVECs) by targeting CREB. Western blot (WB) bands and quantitative analysis determined the expressions of eNOS/AKT pathway-related proteins in MGO-induced HUVECs after treatment with control, insulin (Ins), MGO, MGO+Ins, MGO+miR-450a-5p mimic+negative control (NC), MGO+Ins+mimic+NC, MGO+mimic+CREB, or MGO+Ins+mimic+CREB. ^^$p<0.001$, vs. Control; **$p<0.001$, vs. MGO+mimic+NC; $^{\#\#}p<0.001$, vs. MGO+mimic+CREB. $n=3$.

From *in vitro* cell experiments, this paper discovered that MGO could not only enhance the activity of HUVECs, but also promote cell invasion and fat formation, which was consistent with a previous report (21). Interestingly, the over-expression of miR-450a-5p could reverse the actions of MGO in HUVECs, reduce cell activity, and inhibit cell migration and fat accumulation, suggesting that miR-450a-5p could improve MGO-induced cell damage. It has also been verified that the over-expression of miR-450 observably reduced the proliferation and invasion of lung cancer cells and controlled the growth of tumors (22). Moreover, miR-450a-5p also regulated cell apoptosis by blocking cell cycle and up-regulated miR-450a-5p has an inhibitory effect in the invasion of ovarian cancer cells (23). These findings further suggest that up-regulated miR-450a-5p could alleviate cell deterioration and could be used in treatment of related diseases.

As for the therapy of DM, insulin is the most frequent used drug in the treatment of the disease. Unsatisfactorily, the continuous accumulation of MGO can cause the occurrence and development of insulin resistance in the body (24). In related pathways, insulin has the function of protecting endothelial cells via modulating the activation of eNOS/AKT pathway (25). Concretely, eNOS is an endothelial nitric oxide synthase and can directly affect the ability of endothelial cells to synthesize NO (26). The phosphorylation of AKT activates eNOS, thereby promoting the production of NO and maintaining the normal function of endothelial cells (27). Insulin has the effect of activating eNOS/AKT pathway and promoting the release of NO, thus preventing endothelial cells from damage, which is the same as the results in the current study. However, we also found that MGO inhibited insulin-mediated eNOS/AKT pathway activation, whereas up-regulated miR-450a-5p eliminated the resistance of MGO to insulin, indicating that miR-450a-5p could reverse the effect on insulin resistance mediated by MGO.

Prediction tools and double-luciferase reporter analysis found that CREB had a binding site with miR-450a-5p and CREB was the target gene for miR-450a-5p. Furthermore, miR-450a-5p reversed the effect of MGO on promoting CREB. In the past, research mainly focused on the

function of CREB in the nervous system, and it is known that CREB is widely involved in the biological functions including learning and memory regulation (28). In recent years, researchers demonstrated that activated CREB can promote the proliferation and migration of endothelial cells (29). In addition, activated CREB in the liver promotes hepatic insulin resistance and breaks glucose balance by promoting the CREB Coactivator 2 (CRTC2) activity (30). In this study, we found that CREB obviously suppressed the phosphorylation of eNOS and AKT, suggesting that CREB had an activation effect on the eNOS/AKT pathway. In related studies, Niwano et al. (31) also reported that CREB competitively bound to the cAMP/ATF reactive element to regulate eNOS gene expression in endothelial cells. These finding indicate that miR-450a-5p might relieve MGO-induced insulin resistance via targeting CREB.

In conclusion, the expression of miR-450a-5p is decreased obviously in endothelial cells under the conditions of high-glucose and 500, 1000 μmol/L MGO. In vitro cell experiments show that MGO could not only increase the activity of endothelial cells, but also accelerate cell migration and fat accumulation, which however, could be reversed by up-regulated miR-450a-5p. Moreover, MGO inhibits eNOS/AKT pathway activation and NO release mediated by insulin. Nevertheless, up-regulated miR-450a-5p eliminates the resistance of MGO to insulin via targeting CREB, thus, miR-450a-5p might be a potential therapeutic target to improve MGO-induced insulin resistance.

Acknowledgments

Not applicable.

Potential Conflict of Interest

The authors have no conflicting financial interest.

References

1. Czech MP. Insulin action and resistance in obesity and type 2 diabetes. Nat Med 2017;23:804-814
2. Shamsaldeen YA, Mackenzie LS, Lione LA, Benham CD. Methylglyoxal, a metabolite increased in diabetes is associated with insulin resistance, vascular dysfunction and neuropathies. Curr Drug Metab 2016;17:359-367
3. Matafome P, Rodrigues T, Sena C, Seiça R. Methylglyoxal in metabolic disorders: facts, myths, and promises. Med Res Rev 2017;37:368-403
4. Nigro C, Raciti GA, Leone A, Fleming TH, Longo M, Prevenzano I, Fiory F, Mirra P, D'Esposito V, Ulianich L, Nawroth PP, Formisano P, Beguinot F, Miele C. Methylglyoxal impairs endothelial insulin sensitivity both in vitro and in vivo. Diabetologia 2014;57:1485-1494
5. Hanssen NMJ, Scheijen JLJM, Jorsal A, Parving HH, Tarnow L, Rossing P, Stehouwer CDA, Schalkwijk CG. Higher plasma methylglyoxal levels are associated with incident cardiovascular disease in individuals with type 1 diabetes: a 12-year follow-up study. Diabetes 2017;66:2278-2283
6. Nigro C, Leone A, Raciti GA, Longo M, Mirra P, Formisano P, Beguinot F, Miele C. Methylglyoxal-Glyoxalase 1 balance: the root of vascular damage. Int J Mol Sci 2017;18:E188
7. Wang XJ, Ma SB, Liu ZF, Li H, Gao WY. Elevated levels of α-dicarbonyl compounds in the plasma of type II diabetics and their relevance with diabetic nephropathy. J Chromatogr B Analyt Technol Biomed Life Sci 2019;1106-1107:19-25
8. Kim J, Lee YM, Kim CS, Sohn E, Jo K, Shin SD, Kim JS. Ethyl pyruvate prevents methyglyoxal-induced retinal vascular injury in rats. J Diabetes Res 2013;2013:460820
9. Maessen DE, Stehouwer CD, Schalkwijk CG. The role of methylglyoxal and the glyoxalase system in diabetes and other age-related diseases. Clin Sci (Lond) 2015;128:839-861
10. Zendjabil M, Favard S, Tse C, Abbou O, Hainque B. [The microRNAs as biomarkers: what prospects?]. C R Biol 2017; 340:114-131. French
11. Tiwari J, Gupta G, de Jesus Andreoli Pinto T, Sharma R, Pabreja K, Matta Y, Arora N, Mishra A, Sharma R, Dua K. Role of microRNAs (miRNAs) in the pathophysiology of diabetes mellitus. Panminerva Med 2018;60:25-28
12. Li X. MiR-375, a microRNA related to diabetes. Gene 2014; 533:1-4
13. Zhang Y, Yu M, Dai M, Chen C, Tang Q, Jing W, Wang H, Tian W. miR-450a-5p within rat adipose tissue exosome-like vesicles promotes adipogenic differentiation by targeting WISP2. J Cell Sci 2017;130:1158-1168
14. Mirhashemi F, Scherneck S, Kluth O, Kaiser D, Vogel H, Kluge R, Schürmann A, Neschen S, Joost HG. Diet dependence of diabetes in the New Zealand Obese (NZO) mouse: total fat, but not fat quality or sucrose accelerates and aggravates diabetes. Exp Clin Endocrinol Diabetes 2011;119: 167-171
15. Rao X, Huang X, Zhou Z, Lin X. An improvement of the 2^(-delta delta CT) method for quantitative real-time polymerase chain reaction data analysis. Biostat Bioinforma Biomath 2013;3:71-85
16. Voziyan P, Brown KL, Chetyrkin S, Hudson B. Site-specific AGE modifications in the extracellular matrix: a role for glyoxal in protein damage in diabetes. Clin Chem Lab Med 2014;52:39-45
17. Schalkwijk CG. Vascular AGE-ing by methylglyoxal: the past, the present and the future. Diabetologia 2015;58:1715-1719
18. Liu H, Zhang N, Tian D. MiR-30b is involved in methylglyoxal-induced epithelial-mesenchymal transition of peritoneal mesothelial cells in rats. Cell Mol Biol Lett 2014;19: 315-329
19. Nigro C, Mirra P, Prevenzano I, Leone A, Fiory F, Longo M, Cabaro S, Oriente F, Beguinot F, Miele C. miR-214-Dependent increase of PHLPP2 levels mediates the impair-

ment of insulin-stimulated akt activation in mouse aortic endothelial cells exposed to methylglyoxal. Int J Mol Sci 2018;19:E522
20. Li SS, Wu Y, Jin X, Jiang C. The SUR2B subunit of rat vascular KATP channel is targeted by miR-9a-3p induced by prolonged exposure to methylglyoxal. Am J Physiol Cell Physiol 2015;308:C139-C145
21. Ying C, Sui-Xin L, Kang-Ling X, Wen-Liang Z, Lei D, Yuan L, Fan Z, Chen Z. MicroRNA-492 reverses high glucose-induced insulin resistance in HUVEC cells through targeting resistin. Mol Cell Biochem 2014;391:117-125
22. Wang X, Peng B, Xu C, Gao Z, Cao Y, Liu Z, Liu T. BDNF-ERK1/2 signaling pathway in ketamine-associated lower urinary tract symptoms. Int Urol Nephrol 2016;48:1387-1393
23. Jia H, Xiaojuan L, Li Y, Jiarui Z, Qiao Z, Xinyi L, Miao L, Yanhong L. The effect of miR-450a-5p on the biological behavior of serous ovarian cancer SKOV3 cells. Modern Oncol 2015;7:829-896
24. Memon MA, Khan RN, Riaz S, Ain QU, Ahmed M, Kumar N. Methylglyoxal and insulin resistance in berberine-treated type 2 diabetic patients. J Res Med Sci 2018;23:110
25. De Nigris V, Pujadas G, La Sala L, Testa R, Genovese S, Ceriello A. Short-term high glucose exposure impairs insulin signaling in endothelial cells. Cardiovasc Diabetol 2015;14:114
26. Farah C, Kleindienst A, Bolea G, Meyer G, Gayrard S, Geny B, Obert P, Cazorla O, Tanguy S, Reboul C. Exercise-induced cardioprotection: a role for eNOS uncoupling and NO metabolites. Basic Res Cardiol 2013;108:389
27. Li JB, Wang HY, Yao Y, Sun QF, Liu ZH, Liu SQ, Zhuang JL, Wang YP, Liu HY. Overexpression of microRNA-138 alleviates human coronary artery endothelial cell injury and inflammatory response by inhibiting the PI3K/Akt/eNOS pathway. J Cell Mol Med 2017;21:1482-1491
28. Wang L, Hu XH, Huang ZX, Nie Q, Chen ZG, Xiang JW, Qi RL, Yang TH, Xiao Y, Qing WJ, Gigantelli G, Nguyen QD, Li DW. Regulation of CREB functions by phosphorylation and sumoylation in nervous and visual systems. Curr Mol Med 2017;16:885-892
29. de Jesus DS, DeVallance E, Li Y, Falabella M, Guimaraes D, Shiva S, Kaufman BA, Gladwin MT, Pagano PJ. Nox1/Ref-1-mediated activation of CREB promotes Gremlin1-driven endothelial cell proliferation and migration. Redox Biol 2019;22:101138
30. Hogan MF, Ravnskjaer K, Matsumura S, Huising MO, Hull RL, Kahn SE, Montminy M. Hepatic insulin resistance following chronic activation of the CREB coactivator CRTC2. J Biol Chem 2015;290:25997-26006
31. Niwano K, Arai M, Koitabashi N, Hara S, Watanabe A, Sekiguchi K, Tanaka T, Iso T, Kurabayashi M. Competitive binding of CREB and ATF2 to cAMP/ATF responsive element regulates eNOS gene expression in endothelial cells. Arterioscler Thromb Vasc Biol 2006;26:1036-1042